

Rapid Communications

Rapid Communications are intended for the accelerated publication of important new results and are therefore given priority treatment both in the editorial office and in production. A Rapid Communication in Physical Review B should be no longer than 4 printed pages and must be accompanied by an abstract. Page proofs are sent to authors.

Faraday spectroscopy in diluted-magnetic-semiconductor superlattices

M. Kohl, M. R. Freeman, J. M. Hong, and D. D. Awschalom

IBM Thomas J. Watson Research Center, P.O. Box 218, Yorktown Heights, New York 10598

(Received 10 October 1990)

We investigate the wavelength and magnetic-field dependence of the Faraday rotation in $\text{Cd}_{1-x}\text{Mn}_x\text{Te}/\text{CdTe}$ superlattices in order to probe the strength of the spin-exchange interaction between the excited carriers and the Mn^{2+} ions in these systems. Using a modulation technique we are able to optically record changes of the density of aligned Mn^{2+} spin states $\langle S_z \rangle$ in the order of $\langle S_z \rangle / S_{\text{sat}} = 6 \times 10^{-5}$, where S_{sat} is the saturation density. We observe a steplike behavior at the absorption edge reflecting the density of states and a strong excitonic resonance, which is difficult to resolve by conventional spectroscopic methods like photoluminescence excitation or transmission spectroscopy. With decreasing barrier width L_B we observe below $L_B = 4$ nm a decrease of the strength of the spin-exchange interaction indicating the effects of reduced dimensionality.

Dilute magnetic semiconductors (DMS's) are ideal systems to study magneto-optical effects, since a strong spin-exchange interaction is present between the charge carriers of a host semiconductor and intentionally doped magnetic ions. The recent development of molecular-beam epitaxy for II-VI materials allows the precisely controlled growth of high-quality DMS's, which opens new possibilities for the study of magnetic phenomena, in particular the effects of changes in dimensionality. As a consequence of the spin-exchange interaction, the spin splitting of the electronic states is enhanced in an applied magnetic field, or equivalently, the difference between the indices of refraction corresponding to the two circular polarizations of positive and negative helicity is increased. This effect is particularly pronounced for DMS systems so that the polarization direction of light passing through a film of such a material can perform a considerable rotation (on the order of 10^5 deg/Tcm) before leaving the sample. This so-called giant Faraday effect^{1,2} has been used to examine a number of interesting physical phenomena, including the investigation of phase transitions between the spin-glass phase and the paramagnetic phase of DMS systems.³ In addition, time-resolved Faraday-rotation measurements allowed the direct observation of the formation and evolution of magnetic polarons.⁴ Here we use the Faraday effect, measured by a differential experimental technique, as a sensitive tool required to perform spectroscopy of spin densities in quantum-confined DMS systems.

In the present paper we focus on optical-transmission measurements of the static Faraday rotation in $\text{CdTe}/\text{Cd}_{1-x}\text{Mn}_x\text{Te}$ superlattice (SL) systems. In these systems only the $\text{Cd}_{1-x}\text{Mn}_x\text{Te}$ barrier layers are magnet-

ic. The strength of the magneto-optical phenomena, which are determined by the spin-exchange interaction of the optically excited carriers with the Mn^{2+} ions, thus depends only on the fraction of the electronic wave function which penetrates into the barrier layer. This may be varied by changing the well width or the carrier energy. In particular, interesting questions about the dimensionality dependence of the spin-exchange interaction and the effects of quantum confinement can be studied by changing the width of the $\text{Cd}_{1-x}\text{Mn}_x\text{Te}$ barrier layers. We are able to monitor the electronic density of states in the confined systems by tuning the wavelength of the exciting laser light and to estimate the density of the aligned Mn^{2+} spin states by magnetic-field-dependent Faraday-rotation measurements.

A series of SL samples with $\text{Cd}_{1-x}\text{Mn}_x\text{Te}$ barrier widths L_B ranging from $L_B = 8$ to $L_B = 2$ nm and fixed well widths of 8.6 nm are grown by molecular-beam epitaxy on GaAs substrates with a 150-nm CdTe buffer layer. The number of SL layers is chosen to keep the total thickness of $\text{Cd}_{1-x}\text{Mn}_x\text{Te}$ material fixed at 200 nm. The magnetic dilution is $x = 0.23$ for all samples. The samples are characterized by reflection high-energy electron-diffraction (RHEED) measurements during the growth and later on by x-ray diffraction and low-temperature photoluminescence.⁵ For the transmission experiments the substrate is partly removed by wet-etching techniques. The samples are mounted in a magneto-optical cryostat in Faraday configuration and cooled to temperatures between 1.2 and 5 K. A frequency-doubled Nd-YAG laser (where YAG is yttrium aluminum garnet) synchronously pumps a wavelength-tunable dye laser using Pyridine 2 as a dye to produce excitation wavelengths in the range be-

tween 720 and 800 nm. In order to highly resolve the Faraday rotation of the SL samples we modulate the magnetic field by operating a small coil of superconducting Nb-Ti wire locally in the vicinity of each sample with alternating current and use a phase-sensitive detection scheme. The static external field is applied in the range between $B=0$ and 4 T. A major advantage of this method is its sensitivity only to the magnetic activity in the sample in contrast to small field and energy-dependent polarization changes from neighboring optical components. The peak amplitude of the modulated field, which is parallel to the main magnetic field, is set between 2.4 and 7.2 mT, the modulation frequency is about 1 kHz. In the detection-beam path we split the beam into its 0° and 90° polarization components and detect them separately with photodiodes. The rotation signal is measured as the difference between the 0° and 90° signal using a lock-in amplifier. In order to obtain maximum sensitivity with this "optical bridge" we set the polarization angle of the incident linearly polarized laser beam to 45° with respect to the plane of incidence. The transmission spectra are simultaneously obtained by recording the absolute intensities at both photodiodes with a second lock-in amplifier. The photoluminescence excitation (PLE) spectra are recorded using a 60-cm monochromator and a photomultiplier.

For the evaluation of the rotation angles of the SL's we calibrate the amplitude of the differential signals of a bulk $\text{Cd}_{0.91}\text{Mn}_{0.09}\text{Te}$ crystal. Figure 1(a) shows the measured bulk-rotation signal obtained by using the optical bridge described above without modulating the magnetic field. In the inset the rotation signal is displayed for a larger range of external fields, which are proportional to the rotation angles. Since we measure the difference between the 0° and 90° polarization components of the transmitted laser beam, the rotation signal is given by

$$I = A \text{abs} \left[\cos \left(\frac{\pi B}{P} + \frac{\pi}{4} \right) - \sin \left(\frac{\pi B}{P} + \frac{\pi}{4} \right) \right] + C, \quad (1)$$

where abs denotes the absolute value, P is the period of the rotation, and B the magnetic field. The factor A is proportional to the intensity of the laser light and the amplitude of the applied ac current and indirectly proportional to the temperature.⁶ The rotation angle is given by $\alpha = \pi B/P$. The term C describes all possible background signals, which are, e.g., caused by current heating or by pickup in the leads. These effects cannot be entirely eliminated, but can be discriminated by recording the $2f$ component of the signal or removing the sample, respectively. By fitting Eq. (1) to the experimental signal, see the solid lines in Fig. 1(a), we obtain for our $150\text{-}\mu\text{m}$ -thick bulk sample a rotation of 865° T^{-1} . In Fig. 1(b) we show the corresponding differential signals obtained by modulating the magnetic-field amplitude with a magnetic coil. In this case the measured curves are the derivatives of the rotation signals shown in Fig. 1(a). This is demonstrated by the solid lines, which are obtained by differentiating Eq. (1). The measurements displayed in Fig. 1(b) are performed with a modulation amplitude of 2.4 mT, which corresponds for the bulk sample to a rotation angle of $\alpha = 2.1^\circ$. The quantitative analysis of the differential sig-

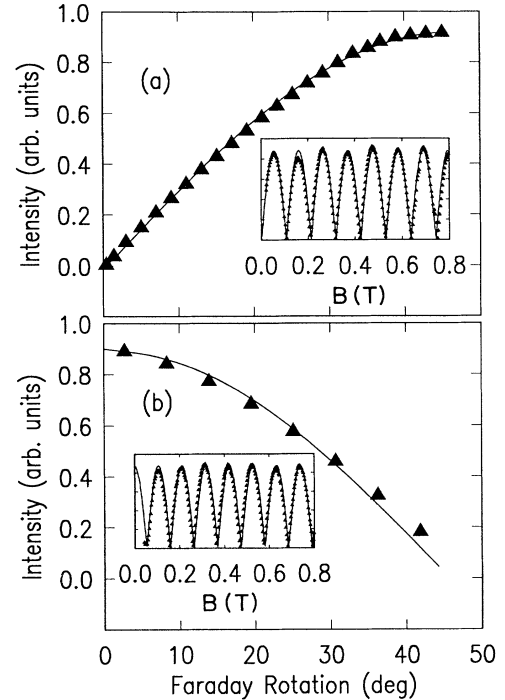


FIG. 1. Faraday-rotation signals of a bulk $\text{Cd}_{0.91}\text{Mn}_{0.09}\text{Te}$ sample of $150\text{ }\mu\text{m}$ thickness obtained (a) without and (b) with modulating the magnetic field by sweeping the external field from 0 to 0.052 T. The insets show the corresponding rotation signals for a larger range of applied magnetic fields. The triangles are measured values, the solid lines are fits calculated by Eq. (1) and the derivative of Eq. (1), respectively. The laser wavelength is 736 nm, which is close to the absorption edge. The laser intensity is 10 W/cm^2 , the temperature is 4.6 K.

nals for the SL's is done by comparing the normalized differential intensities with the corresponding bulk values. For small angles, which we can determine down to about 0.5 mdeg, the differential signal intensities are directly proportional to the rotation angles.

In Fig. 2(a) we show the wavelength dependence of the Faraday rotation of a SL sample with $L_B = 4 \text{ nm}$ for a modulation field of 2.4 mT at zero external field. The corresponding transmission and PLE spectrum are plotted for the same wavelength regime below in Figs. 2(b) and 2(c), respectively. The Faraday-rotation spectrum reveals several striking features.

(i) A nonzero rotation signal of about 6 mdeg is observed between 730 and 750 nm, which corresponds to the energy regime above the onset of the absorption edge. The wavelength position of the absorption edge follows from the transmission spectrum in Fig. 2(b).

(ii) Below the absorption edge at wavelengths longer than 770 nm the rotation signal is essentially zero as expected, since no states can be excited.

(iii) We observe in the PLE spectrum an excitonic transition with a center wavelength of 753 nm. The corresponding photoluminescence transition, which is not shown here, occurs Stokes shifted at 755 nm. At 755 nm the Faraday-rotation signal drops sharply, falls below

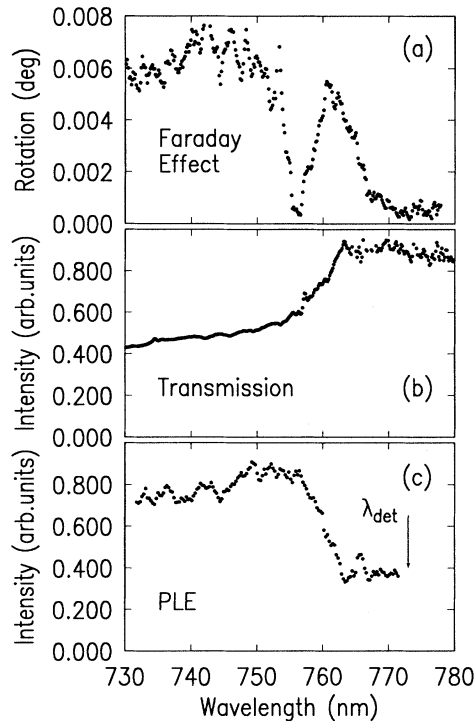


FIG. 2. (a) Wavelength dependence of the Faraday rotation, (b) transmission, and (c) PLE spectrum of a CdTe/Cd_{0.77}Mn_{0.23}Te SL with a well width of 8.6 nm and a barrier width L_B of $L_B = 4$ nm. λ_{det} denotes the detection wavelength. The laser intensity is 10 W/cm², the temperature 4.6 K.

zero, and reverses its sign. This anomalous dispersion behavior is clearly related to the exciton absorption. Since we display the absolute value of the differential signal in Fig. 2(a), a minimum is present at the point of sign reversal. In the transmission spectrum in Fig. 2(b), however, no clear decrease of the intensity of the transmitted light is present, as one would expect at 755 nm in the case of enhanced absorption.

Similar results are obtained for other SL samples having different barrier widths with different rotation angles, which will be compared below. In wavelength-dependent Faraday-rotation measurements on bulk II-VI compounds similar features at the fundamental absorption edge have been reported and interpreted in terms of excitonic resonances.⁷

The measurements in Fig. 2 demonstrate that we are able to very sensitively measure the density of aligned Mn²⁺ spin states in small magnetic fields. A rough estimate of the density of aligned spins at 2.4 mT can be obtained from Fig. 3, which will be discussed below. For $L_B = 4$ nm this yields a value of about $\langle S_z \rangle / S_{sat} = 7 \times 10^{-4}$. Furthermore, the Faraday-rotation spectrum shows a steplike behavior at the absorption edge reflecting the density of states and thus the electronic band structure of the SL systems. The excitonic resonance at 755 nm is, in contrast to the PLE and transmission spectra, only in the Faraday-rotation spectrum highly resolved. The lack of a clear excitonic resonance in the transmission spectrum is

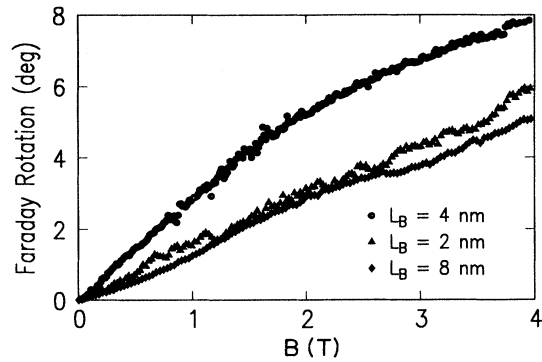


FIG. 3. Magnetic-field dependence of the Faraday rotation excited at 730 nm of three CdTe/Cd_{0.77}Mn_{0.23}Te SL samples with different barrier widths L_B as indicated. The laser intensity is 10 W/cm², the temperature is 4.6 K.

probably due to the broadening of the excitonic band by disorder at the quantum-well interfaces as well as inhomogeneities of the distribution of the Mn²⁺ ions. This can be concluded from the inhomogeneously broadened excitonic transition in the PLE spectrum, which is more than a factor of 2 broader than the width of the region of anomalous dispersion in Fig. 2(a). As a consequence, the center of the excitonic transition in the PLE spectrum does not coincide with the minimum in the Faraday-rotation spectrum.

Temperature-dependent Faraday-rotation measurements between 1.2 and 5 K reveal a T^{-1} behavior of the rotation signal above the band gap, which is expected for isolated spins. The strength of the excitonic resonance shows no clear temperature dependence between 1.2 and about 4 K. However, above 4 K the resonance tends to decrease with increasing temperature. This decrease could be due to the phase transition from a spin-glass state with remaining isolated spins at low temperatures to a paramagnetic state, which occurs for the present Mn²⁺ concentrations at about 4 K. This phase transition has been investigated earlier by magnetic-susceptibility measurements.⁸

In magnetic-field-dependent Faraday-rotation spectra we observe an increase of the rotation angles and a shift of the excitonic-resonance minimum to higher wavelengths. For the SL with $L_B = 4$ nm the minimum shifts linearly by about 2.5 meV T⁻¹ up to $B = 2$ T and then starts to saturate reaching a total shift of about 7 meV at $B = 4$ T. These energy shifts agree with magnetic-field-dependent PL studies on similar SL systems.⁹

In Fig. 3 we show the magnetic-field dependence of the rotation angles obtained for energies above the absorption edge for three different SL samples. As expected, the rotation angles increase linearly at low magnetic fields. The rotation angles obtained from the curves for the different SL samples increase from 6.5×10^4 T⁻¹ cm⁻¹ for $L_B = 8$ nm to 1.3×10^5 T⁻¹ cm⁻¹ for $L_B = 4$ nm. For $L_B = 2$ nm we obtain a rotation of 7.8×10^4 T⁻¹ cm⁻¹. The corresponding value for the bulk sample is 5.8×10^4 T⁻¹ cm⁻¹. Depending on the SL parameters, the curves deviate from this linear dependence at magnetic fields larger than 1 T

due to the saturation of the aligned Mn^{2+} spins, which is also observed for bulk DMS systems.

For our layered structures one would expect that the strength of the spin-exchange interaction directly scales with the penetration of the wave function into the barriers, provided that no dimensionality dependence of the spin-exchange interaction is present. By calculating the wave function for a potential well with finite barriers of widths L_B , we can estimate that the part of the wave function penetrating into the barrier decreases at the wavelength of 730 nm roughly with the ratio 5:4:3 for decreasing L_B in the sequence 8:4:2 nm. Since the number of SL layers in our samples are chosen as 25:50:100, respectively, we consequently expect an increase of the strength of the spin-exchange interaction according to 5:8:12 for the three SL samples in the above sequence. With the inclusion of superlattice effects we expect this increase to be even stronger. If we compare our estimate with the strengths of spin-exchange interactions obtained experimentally by reducing the barrier width from $L_B = 8$ to 4 nm, we obtain very good agreement. However, for the smallest barrier width of $L_B = 2$ nm, the strength of the spin-exchange interaction does not increase as expected, but decreases again. This decrease can be qualitatively explained by the reduced dimensionality of the spin system due to the spin confinement in the barrier layers. For a given carrier the number of neighboring Mn^{2+} spins de-

creases when going from a three-dimensional to a two-dimensional spin system. Therefore, if the dimensions become comparable to the correlation length of the spin-exchange interaction, we expect a decrease of the spin-exchange interaction between the carriers and the Mn^{2+} ions, provided that the spin-exchange interaction between the Mn^{2+} ions is less dimensionality dependent. An earlier investigation of the magnetic susceptibilities χ of our SL samples⁸ showed a similar scaling of χ for decreasing L_B , in agreement with the present results.

In conclusion, we have investigated the wavelength and magnetic-field dependence of the Faraday rotation in diluted magnetic SL's to probe the strength of the spin-exchange interaction in these systems. In order to determine accurately small rotation angles down to less than 1 mdeg we modulate the magnetic field using a phase-sensitive detection scheme. The wavelength-dependent Faraday spectra reflect the behavior of the band structure of the investigated systems. We observe the steplike density of states and a strong excitonic resonance, which is more easily resolved than in conventional PLE and transmission spectra. A comparison of the rotation angles found for decreasing barrier thicknesses L_B reveals a strong deviation from the expected behavior below $L_B = 4$ nm, indicating the crossover of the dimensionality from a three-dimensional to a two-dimensional spin system in the SL structures investigated.

¹J. A. Gaj, R. R. Galazka, and M. Nawrocki, *Solid State Commun.* **25**, 193 (1978).

²For a recent review on the magneto-optical properties of large-gap DMS see, e.g., J. A. Gaj, in *Semiconductors and Semimetals*, edited by J. K. Furdyna and J. Kossut (Academic, Boston, 1988), Vol. 25, p. 275.

³A. Mycielski, C. Rigaux, and M. Menant, *Solid State Commun.* **50**, 257 (1984); E. Kierzek-Pecold, W. Szymańska, and R. R. Galazka, *ibid.* **50**, 685 (1984).

⁴D. D. Awschalom, J.-M. Halbout, S. von Molnar, T. Siegrist, and F. Holtzberg, *Phys. Rev. Lett.* **55**, 1128 (1985).

⁵J. M. Hong, D. D. Awschalom, L. L. Chang, and A. Segmüller,

J. Appl. Phys. **63**, 3285 (1988).

⁶Analytical formulas for the evaluation of the Faraday-rotation angle in the different limits of magnetic concentration and temperature are provided, e.g., in D. U. Bartholomew, J. K. Furdyna, and A. K. Ramdas, *Phys. Rev. B* **34**, 6943 (1986).

⁷P. S. Kireev, L. V. Volkova, and V. V. Volkov, *Sov. Phys. Semicond.* **5**, 1812 (1972) [*Fiz. Tekh. Poluprovodn.* **11**, 2080 (1972)].

⁸D. D. Awschalom, J. M. Hong, L. L. Chang, and G. Grinstein, *Phys. Rev. Lett.* **59**, 1733 (1987).

⁹J. Warnock, A. Petrou, R. N. Bicknell, N. C. Giles-Taylor, D. K. Blanks, and J. F. Schetzina, *Phys. Rev. B* **32**, 8116 (1985).